

A Computational Study of Flow-Induced Plate Flutter as Potential Markers for Sleep Apnea


 Open
Access

 Mohammad Rasidi Rasani^{1,*}, Kiao Inthavong², Jiyuan Tu²
¹ Center for Integrated Design for Advanced Mechanical Systems, Faculty of Engineering and Built Environment, Universiti Kebangsaan Malaysia, 43600 Bangi, Selangor, Malaysia

² School of Aerospace, Mechanical, Manufacturing Engineering, RMIT University, Bundoora, Victoria, 3083, Australia

ARTICLE INFO

Article history:

Received 25 August 2019

Received in revised form 18 October 2019

Accepted 22 October 2019

Available online 28 October 2019

ABSTRACT

Collapse of airway during sleep (sleep apnea) is a disorder that requires expensive and cumbersome sleep tests for its diagnosis, making it unattractive for large-scale detection in the mass population. Acoustic signals from snoring has become an attractive research area for developing inexpensive and non-invasive test for diagnosing sleep apnea. In this article, potential for an alternative apnea detection from snoring acoustic signals is investigated by examining effect of airway obstruction on onset of soft palate snoring or flutter. To that end, this study is concerned with flow-induced vibrations of a cantilever plate inside a two-dimensional, viscous, obstructed channel flow that represents the human pharynx associated with snoring and obstructive sleep apnea syndrome. The soft palate vibrations are examined by coupling a full Navier-Stokes flow solver in an Arbitrary Lagrangian-Eulerian (ALE) description to a thin plate equation of motion. A threshold velocity for initiation of unstable plate vibration was determined for each different occlusion depth, and correlating the two, showed that the critical velocity decreased with increasing occlusion depth. By relating the critical velocity to a breathing cycle, the time for initiation of snoring could help estimate the degree of localized airway occlusion and justify further study for potential non-invasive diagnosis of obstructive airway.

Keywords:

Flutter; Sleep apnea; Fluid-structure interaction; Palatal snoring

Copyright © 2019 PENERBIT AKADEMIABARU - All rights reserved

1. Introduction

Vibrations of structures induced by flow of fluids occurs in many phenomena ranging from environmental, biological to engineering applications. Not surprisingly, flow-induced vibrations have attracted intensive research especially flow-induced vibrations of cylinders [1-3], plates [4-6], membranes or flags [7,8], all of which represent canonical problems that may facilitate understanding of real-world phenomena. Some of the many current topics in this field include studies to exploit flow-induced vibrations to harvest energy [9-11] and investigations on fluid elastic instability such as flutter or galloping, that may lead to unfavorable dynamic structural response

* Corresponding author.

E-mail address: rasidi@ukm.edu.my (Mohammad Rasidi Rasani)

[7,12]. In particular, the latter topic is also prevalent in human physiology and one of the primary examples is their role in biomechanics of snoring.

Obstructive sleep apnea involves partial or complete occlusion of human upper airway during sleep, which compromises sleep quality and reduces oxygen saturation in the blood. Although snorers may not necessarily have sleep apnea, most apnea patients experience snoring - indicating a potential relationship between the two conditions. Indeed, people who snore are more predisposed to obstructive sleep apnea [13,14], which have also been linked to high blood pressure and cardiac failures [15]. Biomechanics of snoring are closely associated to flow-induced unstable vibrations of the soft palate and the upper airway walls. At adequately high velocities, flow-induced vibration of the soft palate becomes unstable – typically via flutter, which seems to be the most common mechanism for snoring [14].

Flow through channels with internal cantilever plates have been studied extensively to model physical conditions such as flow-induced flutter and soft palate snoring [16]. The upper airway can be idealized as a channel flow where an obstruction mimics a narrowed opening that may be caused by anatomical tissue build-up or collapse of the airway tissues as low pressure develops due to venturi effects. Sleep apnea patients have been shown to have narrower opening in the oropharynx [17-19], affecting pharyngeal compliance [20].

Aurégan and Depollier [21] analytically and experimentally investigated flow around flexible beam that is cantilevered inside a channel, to represent soft palate snoring and showed a flutter-type instability was involved. While Huang [14], analytically modeled channel flow with a flexible cantilever plate and showed circulatory part of the fluid loading (as a result of reaction to trailing wake vortices), was accountable for destabilizing the system vibrations. Using similar linear theodorsen airfoil theory but in their more recent work, Huang and Zhang [22] analyzed eigenvalue problem of cantilever plate flutter and showed close coupling between first mode vibrations and second mode-induced fluid loading. In another study, Guo and Paidoussis [23] analyzed linear stability of rectangular plate vibrations under various leading and trailing edge boundary conditions, in a non-viscous 2D channel flow. Their results showed that plates supported at both leading and trailing edges, experience instability via a divergence mechanism first before other types of instability modes, due to excessive destabilizing fluid pressures. Tang *et al.*, [24-25] considered non-linear large plate deformation assuming an inextensibility condition in their investigations of flow-induced vibrations of a cantilever plate. Although a separate viscous drag estimation was considered into the plate motion equation, the flow was assumed non-viscous and the applied pressure difference on the plate was determined by employing an unsteady lumped vortex model. Similarly, Shoele and Mittal [26] considered two-dimensional channel flow in their nonlinear eigenvalue analysis of flow-induced plate stability. Although an inviscid flow was assumed, their analytical model showed good agreement to predict flutter.

Balint and Lucey [27] and Tetlow and Lucey [28] instead considered viscous effects in their instability analysis for a cantilever plate vibration in a 2D channel flow. Their results demonstrated that if both top and bottom inlets are open, a flutter instability is generated above a critical or threshold Reynolds number, due to viscous effects instead of time-dependent flow separation at the plate trailing edge. If instead one of the inlets is closed, the plate exhibits instability via a divergence mechanism when a critical velocity is reached. Despite demonstrating lower flow to plate energy exchange, Tetlow and Lucey [29] showed similar flutter instability when the 2D channel is driven by pressure difference instead of velocity-driven flow as applied in Balint *et al.*, [27]'s research. Other related works from this research group included the interaction between a cantilevered-free flexible plate and ideal flow [30] and more recently, stability of a flexible insert in one wall of an inviscid channel flow [31]. Unlike previous studies, Khalili *et al.*, [32] considered

compressible viscous flow in their fluid-structure interaction solver and further analyzed the acoustic pressure signals in the two-dimensional channel-plate model. Their spectrum analysis indicated that the plate oscillation frequency is recognizable when the dominant quarter wave mode harmonics decay sufficiently.

Current sleep tests tend to be costly and cumbersome for diagnosis of sleep apnea, making it impractical for mass screening. Since biomechanics and soft tissues involved with sleep apnea and snoring are similar, acoustic signals from snoring may carry important information concerning the conditions of the pharynx during sleep. Therefore, a number of studies have examined snoring signals as alternative technique for diagnosing sleep apnea [33-38]. However, the variation in onset of snoring against degree of airway obstruction has not been fully investigated as a potential means for non-invasive and inexpensive diagnosis of sleep apnea. In this study, we aim to correlate the onset of flow-induced unstable vibrations of the soft palate with varying degrees of airway obstruction. This paper extends the current results in the literature by investigating the effect of localized obstruction on the stability of a flexible cantilevered plate, representing soft palate dynamics during inhalation. A fluid-structure interaction model is used to explore the relationship between the critical inhalation velocity for onset of palatal snoring and the localized airway obstruction depth, in relation to possible non-invasive sleep apnea diagnosis. Flow around a flexible plate that is cantilevered inside a two-dimensional channel is modeled, with a gradually developing obstruction or narrowing introduced in one of the passages to represent a partially occluded upper airway.

2. Methodology

2.1 Channel and Cantilever Plate Geometry

Flow over a flexible cantilevered plate inside a channel is modeled with an obstruction at the upper passage of the channel (Figure 1 (a)) to represent the upper airway with a localized obstruction (due to perhaps, collapse of the tongue).

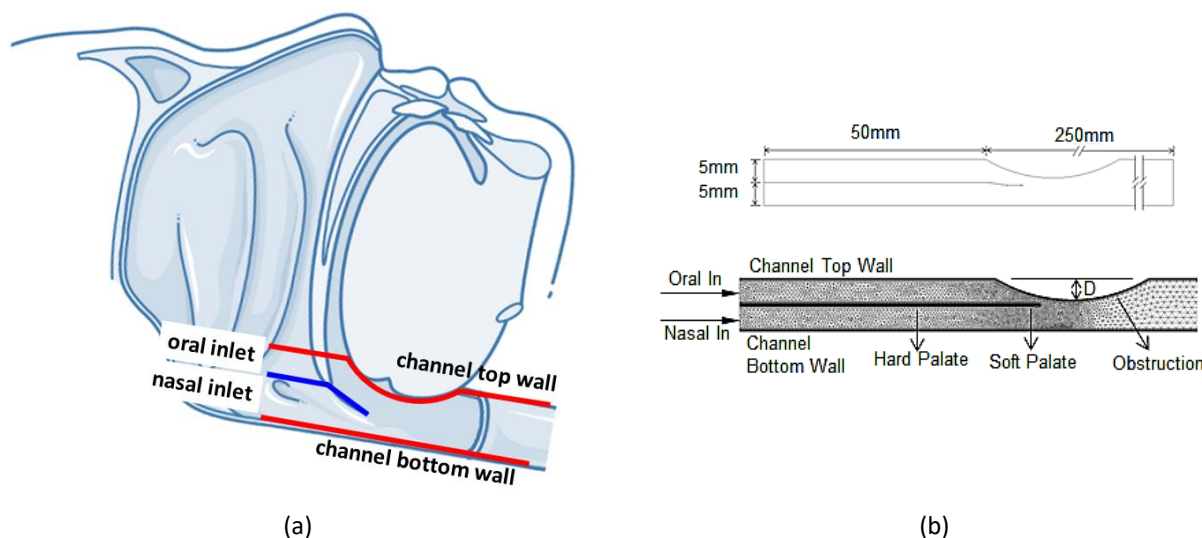


Fig. 1. (a) Idealization of oral and nasal passage through upper airway (adapted from a public domain medical illustration (smart.servier.com) under a creative common license), (b) Computational domain and mesh of the idealized model (D represents obstruction depth)

Adopting the geometry employed in Balint *et al.*, [27]'s study, a channel half-width of 5 mm is idealized, but the upstream span between start of the cantilever plate and inlet boundary is set to 50 mm and the downstream distance to the outlet boundary is 250 mm. This is to provide adequate length for flow to develop before reaching the cantilever plate and prior to channel exit. The length of the blockage is kept constant but its depth, D is varied between 0 - 4 mm. A uniform velocity profile is prescribed at the inlet and we examine the variation in the inlet velocity (U_{crit}) needed for initiation of plate instability, for different D .

2.2 Fluid Model

The two-dimensional, laminar, incompressible, unsteady Navier-Stokes equations are used to account for fluid flow in channel, as shown in Eq. 1 and Eq. 2.

$$\frac{\partial u_i}{\partial t} + (u_j - \tilde{u}_j) \frac{\partial u_i}{\partial x_j} = -\frac{1}{\rho} \frac{\partial p}{\partial x_i} + \frac{\partial}{\partial x_j} \left[\frac{\mu}{\rho} \left(\frac{\partial u_i}{\partial x_j} + \frac{\partial u_j}{\partial x_i} \right) \right] \quad (1)$$

$$\frac{\partial (u_i - \tilde{u}_i)}{\partial x_i} \quad (2)$$

where u_i , \tilde{u}_j and p are the fluid velocities, fluid grid velocities and pressure respectively ($i, j = 1, 2$ represent the 2D cartesian directions), ρ is the constant fluid density and μ represents the fluid dynamic viscosity. To allow fluid mesh deformation, following the motion of the cantilever plate, the Arbitrary Eulerian-Lagrangian (ALE) description is used in Eq. 1 and Eq. 2. The fluid grid velocity is solved using a Laplacian Diffusion model, which can smooth the grid velocity from a value equal to the plate motion velocity at the fluid-plate interface, to zero grid velocity or displacement at the boundaries of the fluid domain.

The channel top and bottom wall, and bisecting 'hard palate' are prescribed as wall boundaries (with no-slip conditions). The outlet is defined with a stress-free boundary condition. The channel length is sufficiently long to allow a fully developed flow towards the cantilever plate. Approaching the 'hard palate', cantilever plate and channel walls, refined boundary layer meshes are defined. Finer meshing is also prescribed in regions at the vicinity of the blockage and at the tip of the cantilever plate (as shown in Figure 1 (b)), where sharper flow gradients are expected.

2.3 Cantilever Plate Model

The cantilever plate dynamics is described by the continuum equation in Eq. 3.

$$\rho_s \frac{\partial^2 q_i}{\partial t^2} = \nabla \cdot \sigma_{ij} + f_i(t) \quad (3)$$

where ρ_s is the structural density, q_i represents the structural displacements, f_i is the external forcing term (obtained from the interfacing fluid pressure and shear) and σ_{ij} is the stress tensor ($i, j = 1, 2$ for 2D structures). The first term on the RHS (right hand side) of Eq. 3 embodies the internal resistive force in the structure, which for a thin plate (of thickness h , elastic modulus E and Poisson ratio ν) under lateral loading, is primarily a function of its bending stiffness, $B = (Eh^3)/12(1 - \nu^2)$. Induced tension in flexible vibrating structures can limit flutter amplitudes [39],

and therefore non-linear large plate deflection may also be accounted in the present study via Eq. 3.

The root of the flexible cantilevered plate is fixed to the ‘hard palate’, while its trailing edge is free.

2.4 Fluid-Structure Coupling

The fluid and structural coupling is implemented by requiring both kinematic and dynamic continuity at the shared fluid-structure interfaces (i.e. compatibility in motion and balance of force respectively). The steady-state solution for each channel inlet velocity is prescribed as the initial condition for their respective transient fluid-structure simulation. Both fluid pressure and shear stresses from the flow solver is communicated to the structural solver and the resulting plate deflection that is estimated from the structural solver is feed backed to the fluid solver, that then effects the displacement of the fluid boundary interfacing the plate. For similar time step sizes, this implies matching structural and fluid velocities at the fluid-structure interface [40,41]. This fluid-structure coupling is implemented via a partitioned framework in ANSYS 14.5.

Considering A_1 and A_2 as the upper and lower plate surfaces respectively, the energy equation for the oscillating cantilever plate may be described as [42,43]

$$\frac{d}{dt} \left(\frac{1}{2} \int_V \rho_s \dot{\mathbf{q}}^2 dV + \frac{1}{2} \int_V \boldsymbol{\sigma} \cdot \boldsymbol{\epsilon} dV \right) = \left(\int_{A_1} \boldsymbol{\sigma}^f \dot{\mathbf{q}} dA + \int_{A_2} \boldsymbol{\sigma}^f \dot{\mathbf{q}} dA \right) - d \int_V \dot{\mathbf{q}}^2 dV \quad (4)$$

$$\frac{1}{2} \int_V \rho_s \dot{\mathbf{q}}^2 dV : \text{Kinetic energy}$$

$$\frac{1}{2} \int_V \boldsymbol{\sigma} \cdot \boldsymbol{\epsilon} dV : \text{Strain energy}$$

$$\int_{A_1} \boldsymbol{\sigma}^f \dot{\mathbf{q}} dA + \int_{A_2} \boldsymbol{\sigma}^f \dot{\mathbf{q}} dA : \text{Rate of aerodynamic work}$$

$$d \int_V \dot{\mathbf{q}}^2 dV : \text{Rate of dissipation}$$

where \mathbf{q} is the displacement vector of the plate, ρ_s is the density of the plate material, $\boldsymbol{\sigma}$ is the plate stress vector, $\boldsymbol{\epsilon}$ represents the plate strain vector, $\boldsymbol{\sigma}^f$ denotes vector of the fluid traction applied on plate surfaces and d represents a damping parameter of the plate (for a case where damping is considered). Therefore, the total kinetic and strain energy of the plate (left hand side of Eq. 4 is induced by the rate of work on the plate imposed by the aerodynamic loading. If this aerodynamic rate of work exceeds the structural damping - yielding a net positive magnitude on the right-hand side of Eq. 4, the total plate energy grows with time. As a result, cantilever plate vibration amplitude increases with time and plate instability ensues.

Vibration characteristics of structures are influenced by a number of physical properties [44]. In the present study, we considered parameters based on the work in Balint *et al.*, [27]’s research, which gives a second mode frequency of 100 Hz for the cantilever plate and conforms with soft palate snoring frequencies between 30-100 Hz reported in previous studies [27]. Table 1 summarizes their values.

Table I
Parameters in the present fluid-structure system

Parameters	Values
Cantilever plate length	8.5 mm
Plate modulus, E	880 MPa
Plate poisson ratio, ν	0.3333
Plate density, ρ_s	2272.73 kg/m ³
Air density, ρ	1.18 kg/m ³
Air dynamic viscosity, μ	1.982 × 10 ⁻⁵ Pa.s

2.5 Preliminary Study

A nominal time step of $t = 5e-4$ s was selected for the simulations, which should be appropriate with the 100 Hz second mode frequency of the plate. To ensure this time step was adequate, a time independence test was performed for case $D = 0$ mm using a time step of $t = 5e-5$ s. Figure 2 (a) shows a slight phase shift in plate response, but otherwise minimal difference between both time steps used - indicating sufficient temporal discretization for the purpose of this study. Each simulation was performed for a total time of $t = 0.05$ s (i.e. 100 time steps).

In order to verify adequate spatial discretization is used in the present model, a simulation (for occlusion depth $D = 4$ mm) was undertaken with finer mesh (as shown in Figure 2 (b)) where the baseline mesh size was halved, giving a total of 67322 elements in comparison to the baseline 20363 number of elements. The tip oscillations between the finer and baseline mesh are found to be very similar suggesting that the results are sufficiently independent from the baseline grid size employed in the present study.

In addition, previous studies have noted that the channel downstream length may affect the fluid resistance and inertance, which would then influence the oscillation period of the flexible plate [27,45]. To evaluate the sensitivity of the cantilever plate dynamics to channel downstream length, another run for case $D = 4$ mm is simulated, but with the downstream length increased by 60% - i.e. to 400 mm (from the baseline 250 mm length employed in all the simulations). Again, both amplitude and frequency response were found to be indistinguishable between both cases (Figure 2 (c)), indicating the baseline model with 250 mm downstream length, is adequately not sensitive to channel downstream lengths.

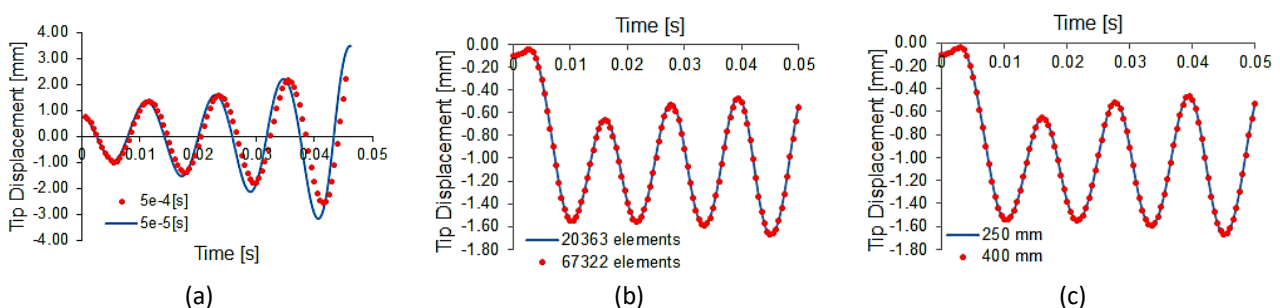


Fig. 2. Model verification: (a) temporal sensitivity test, (b) grid independence test, (c) channel length sensitivity test

3. Results and Discussion

3.1 Critical Inhalation Velocity

We simulated a number of cases with different channel inlet velocities (U_{in}) to estimate the critical inhalation velocity for initiation of plate instability, for the considered obstruction depths (D)

= 0 mm, 2 mm and 4 mm). The plate oscillation history was observed and instability of the flexible plate was identified if amplitude of plate tip oscillation increased over time. Figure 3 demonstrates contours of the streamwise velocity component and corresponding cantilever plate deflections at the same time instances for $U_{in} = 0.5$ m/s and 0.8 m/s at obstruction depth of $D = 4$ mm. The cantilever plate deformation for $U_{in} = 0.8$ m/s are more noticeable and show increasing amplitude over time - suggesting plate instability, while for $U_{in} = 0.5$ m/s consistent deflection in amplitudes are generated.

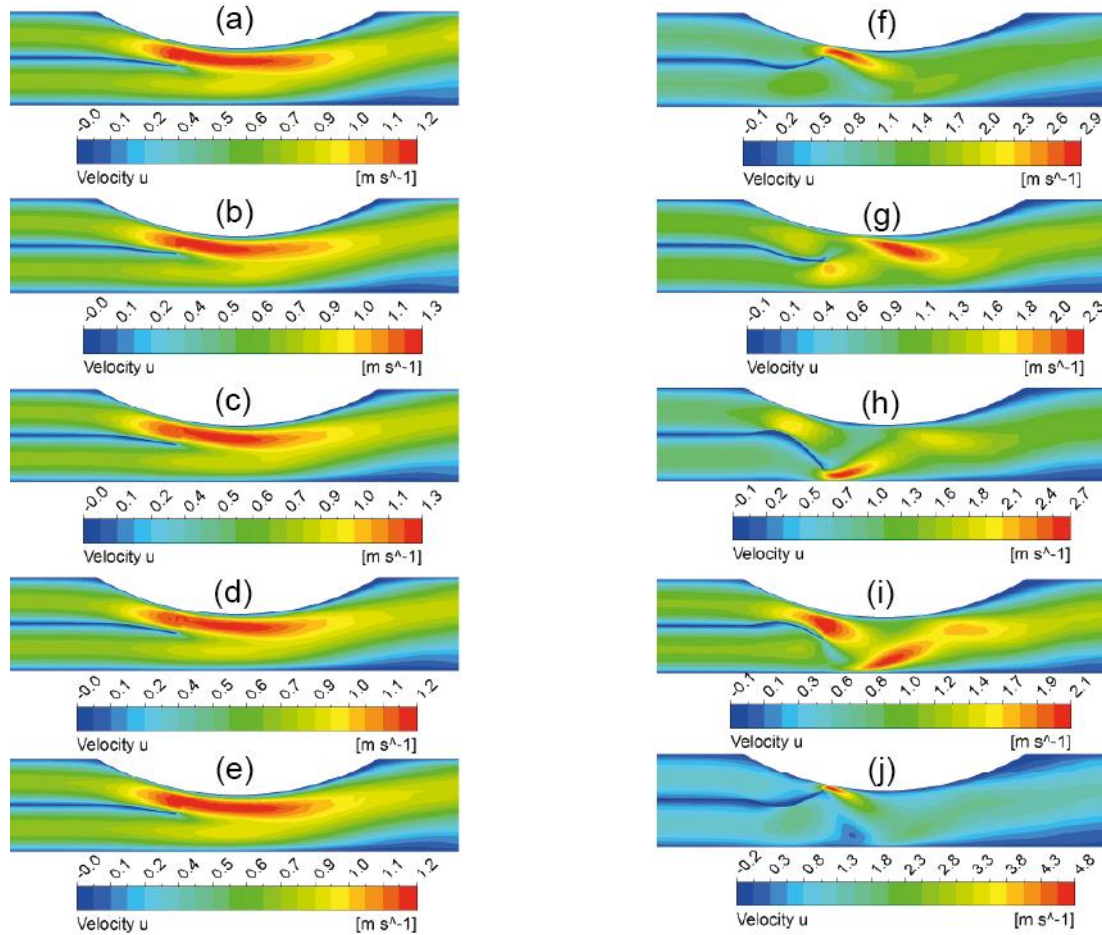


Fig. 3. Instantaneous velocity comparison (at similar instances) due to cantilever plate motion for channel occlusion depth $D = 4$ mm; (a)-(e) for $U_{in} = 0.5$ m/s and (f)-(j) for $U_{in} = 0.8$ m/s. Note the increased proximity of cantilever plate tip to channel wall in (j) compared to (f) for case $U_{in} = 0.8$ m/s

We remark that in previous studies, inspiratory volumetric flow rate of snorers during sleep may fall in the range of 0.37 ± 0.10 L/s [46] and that average hydraulic diameter of nasal posterior airway space may measure approximately 26.5 mm (in control subjects) and 15.4 mm (in apnea subjects) [47]. Combining these parameters yield an inflow velocity in the range between 0.7 - 2.0 m/s, within which inlet velocities are applied in the present study.

To identify the critical velocity, tip amplitude over time was plotted for varying inlet velocities by increments of ± 0.1 m/s (for example, $U_{in} = 0.6$ m/s and 0.7 m/s). Figure 4 (a) shows tip amplitude growth for inlet velocity $U_{in} = 0.7$ m/s, while for $U_{in} = 0.6$ m/s, it decays over time. The critical velocity was also evaluated for obstruction depths of $D = 2$ mm, and $D = 0$ mm by simulating a range of different velocities and checking for velocity when tip deflection growth first occurs.

For an obstruction depth of 2 mm obstruction ($D = 2\text{ mm}$), Figure 4(b) shows the tip amplitude decays for inlet velocity of $U_{in} = 1.0\text{ m/s}$, but grows for $U_{in} = 1.1\text{ m/s}$. Similarly, in Figure 4 (c) for $D = 0\text{ mm}$, the tip amplitude decays for $U_{in} = 1.3\text{ m/s}$, but grows for $U_{in} = 1.5\text{ m/s}$. The results suggest that for channel with occlusion depths of $D = 0, 2, 4\text{ mm}$, the corresponding critical velocities for initiation of plate instability are respectively: $U_{crit} = 1.4\text{ m/s} \pm 0.1\text{ m/s}$, $1.05 \pm 0.05\text{ m/s}$ and $0.65 \pm 0.05\text{ m/s}$.

Correlating the critical velocities against obstruction depths, shows the critical velocity has a negative linear relationship with increasing obstruction depth. The coefficient of determination (R^2) in Figure 4 (d) represents the extent of the variance in the critical velocity that is predictable from the obstruction depth, which for a linear regression is the square of the correlation between these variables. The closeness of the R^2 value to 1.0 shows strong correlation between U_{crit} and D of the linear equation shown in Figure 4 (d).

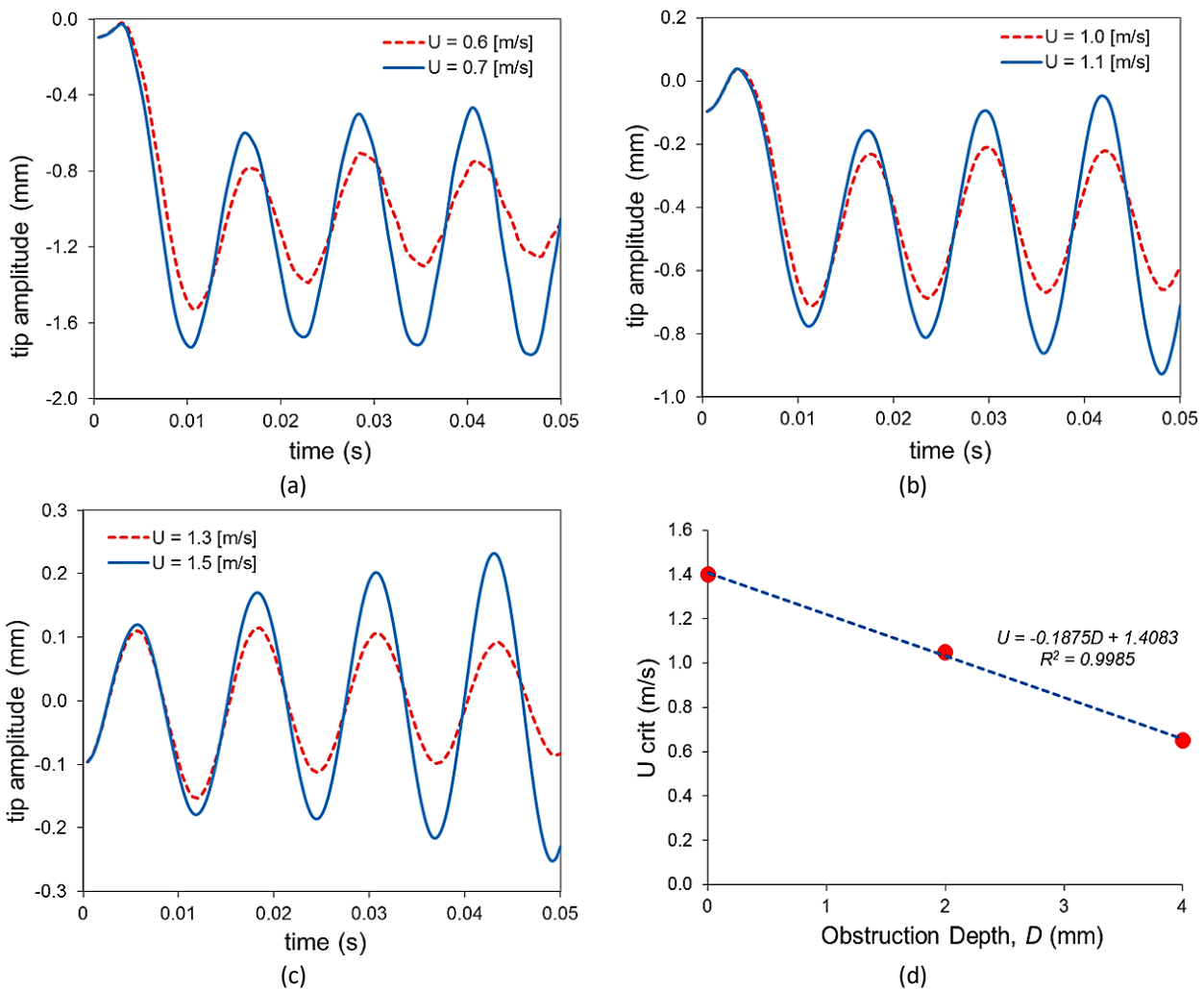


Fig. 4. Oscillation history of plate tip for various inlet velocities under various occlusion depth: (a) $D = 4\text{ mm}$, (b) $D = 2\text{ mm}$, (c) $D = 0\text{ mm}$, (d) Critical velocity variation with obstruction depth showing a linear correlation

3.2 Instability Mechanism

The tip amplitudes or deflection pattern show a bias in the plate oscillation to deflect away from the blockage, i.e. tending towards the lower wall, and vibrate about that position. This is

caused by the originally greater flow resistance in the upper passage - suggesting higher pressure gradient on the upper channel in contrast to the lower channel. A negative lift (downforce) first acts on the cantilever plate before the plate oscillation occurs, producing a phase difference between lift force and plate oscillation. This is similar to features of flutter-type instability, where maximum positive lift coincides with minimum (negative) displacement of the plate motion, providing irreversible feed of energy at the appropriate moment from the flow to the oscillating structure. Unlike instability driven by quasi-static divergence mechanism, which occur when fluid tractions (σ^f) exceeds the plate resisting internal traction, positive rate of aerodynamic work in Eq. 4 may also arise despite lower fluid traction values, provided that σ^f is out-of-phase with the plate oscillation (\mathbf{q}) [27].

3.3 Discussion

Soft palate snoring is characterized through soft palate instability, with oscillation amplitudes growing over time. The cantilever plate example demonstrated that onset of soft palate instability (i.e. snoring) is a function of the breathing-in velocity. The presence of occlusion in the proximity of the soft palate lowers the threshold velocity that initiates unstable soft palate vibrations and thus snoring. Considering that inhalation velocity accelerates with a sinusoidal profile, earlier initiation of snoring is predicted for persons with higher degree of occlusion in the proximity of soft palate. By correlating this critical inlet velocity with time from an inhalation flow curve, we may estimate the degree of occlusion in the region of the soft palate. When this data is compared with acoustic recordings of a snoring patient (e.g. in reference [38]), an estimate for the degree of occlusion in the proximity of the soft palate can be found, based on elapsed time taken from beginning of inhalation to onset of snoring (Δt in Figure 5).

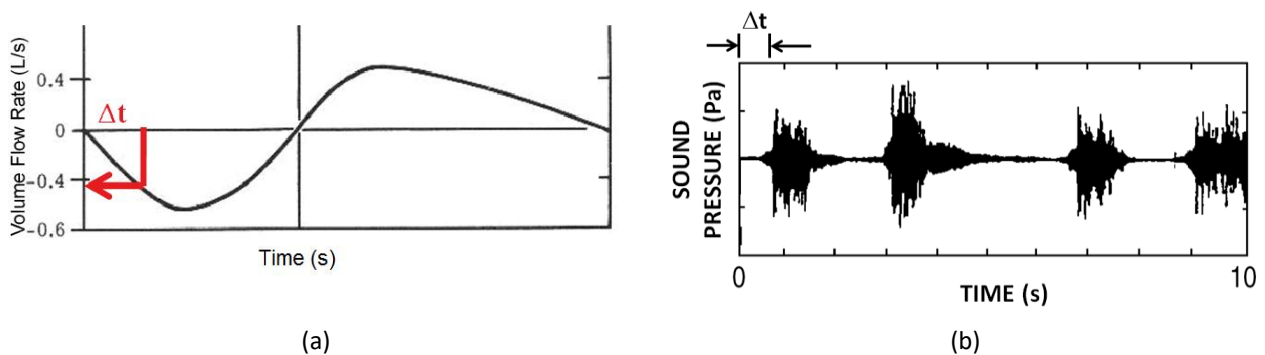


Fig. 5. (a) Sample of typical breathing flow curve [48], (b) Sample of acoustic recording during sleep [38]. Elapsed time to onset of snoring Δt , correlates to critical inhalation velocity in flow curve, and therefore varies with degrees of airway obstruction

While the present work is based on idealized airway geometry and modeling assumptions, when combined with recent clinical studies the results provide deeper insight to onset of unstable soft palate oscillations. In a clinical study, subjects with severe sleep apnea were reported to show more regular snores of time interval $< 1s$ in comparison to healthy sleepers [33]. This implies a smaller time difference between snoring episodes, indicating a tendency for snoring to start earlier as critical inhalation velocity for initiation of snoring is lowered when localized occlusion or narrowing is present in the airway. In another study, apneic patients were observed to have wider variance in the time between snoring episodes in comparison to benign snorers [34]. As many sleep apnea patients are reported with more compliant airways, larger variation on occlusion or opening

size of the airway is expected under the fluctuating negative and positive pressures developed during breathing cycles. This may be due to lack in control of airway muscle tone or buildup of softer fatty tissues. As a result, varying threshold velocity for initiation of snoring is expected in these cases, leading to large variance of elapsed time between snoring.

4. Conclusions

Soft palate snoring was modelled by idealizing flow-induced vibration of a flexible cantilever plate inside a channel. The instability of this flexible plate under the influence of localized occlusion was investigated, showing a near-linear reduction in threshold inlet velocity required for onset of unstable plate vibrations, with increasing occlusion depth. In turn, with shallower occlusion depth, the critical inlet velocity is linearly higher. The characteristics of the plate instability indicates a flutter mechanism is involved. Linking the correlation between the critical velocity and occlusion depth to the breathing cycle, indicated potential measurement variables that could be exploited for non-invasive diagnosis of airway obstruction - either by measurement of time interval from start of inhalation to onset of snoring, or perhaps time interval between snoring episodes. Future simulations for nasal- and oral-only inhalation may need to be explored. Another potential area that needs to be further considered is the response of the soft palate after potentially contacting the bounding pharynx (or in this case, channel) walls and how it may affect the soft palate snoring signals.

Acknowledgement

The authors would like to gratefully acknowledge the financial support provided by the Australian Research Council (Project ID: DP120103958), and the assistance of resources provided by the Malaysian Ministry of Higher Education research grant FRGS/1/2018/TK03/UKM/02/5.

References

- [1] Vandiver, J. Kim, Leixin Ma, and Zhibiao Rao. "Revealing the effects of damping on the flow-induced vibration of flexible cylinders." *Journal of Sound and Vibration* 433 (2018): 29-54.
- [2] Raeesi, A., S. Cheng, and D.-K. Ting. "Some insight into the wind-induced vibration of stay cables in the context of rigid static inclined circular cylinder." *Journal of Applied Fluid Mechanics* 5, no. 2 (2012): 99-112.
- [3] Syamsul Azry Md Esa, Wan Mohd. Arif Aziz Japar, and Nor Azwadi Che Sidik. "Design and Analysis of Vortex Induced Vibration (VIV) Suppression Device." *CFD Letters* 11, no. 2 (2019): 66-80.
- [4] Pigolotti, Luca, Claudio Mannini, and Gianni Bartoli. "Destabilizing damping effect on flat-plate vibrations due to flow-induced flutter." *Procedia engineering* 199 (2017): 790-795.
- [5] Purohit, Ashish, Ashish K. Darpe, and S. P. Singh. "Influence of flow velocity and flexural rigidity on the flow induced vibration and acoustic characteristics of a flexible plate." *Journal of Vibration and Control* 24, no. 11 (2018): 2284-2300.
- [6] Atheer Raheem Abdullah, Wajeeh Kamal Hasan, and Mustafa Abdulsalam Mustafa. "Numerical Investigation of Hydrostatic Pressure on Free Vibrating Rectangular Cantilever Plates Partially Submerged in Viscous Media." *Journal of Advanced Research in Fluid Mechanics and Thermal Sciences* 60, no. 1 (2019): 1-14.
- [7] Alben, Silas. "Flag flutter in inviscid channel flow." *Physics of Fluids* 27, no. 3 (2015): 033603.
- [8] Abderrahmane, Hamid Ait, Michael P. Paidoussis, Mohamed Fayed, and Hoi Dick Ng. "Nonlinear dynamics of silk and Mylar flags flapping in axial flow." *Journal of Wind Engineering and Industrial Aerodynamics* 107 (2012): 225-236.
- [9] Orrego, Santiago, Kouros Shoele, Andre Ruas, Kyle Doran, Brett Caggiano, Rajat Mittal, and Sung Hoon Kang. "Harvesting ambient wind energy with an inverted piezoelectric flag." *Applied energy* 194 (2017): 212-222.
- [10] Javed, Ali, Kamal Djidjeli, A. Naveed, and J. T. Xing. "Low Reynolds Number Effect on Energy Extraction Performance of Semi-Passive Flapping Foil." *Journal of Applied Fluid Mechanics* 11, no. 6 (2018).

- [11] Methal, Zinnyrah, Mohamed Sukri Mat Ali, Nurshafinaz Mohd Maruai, and Rasli Abd Ghani. "Microwatt Energy Harvesting by Exploiting Flow-Induced Vibration." *Journal of Advanced Research in Fluid Mechanics and Thermal Sciences* 47, no. 1 (2018): 25-34.
- [12] Mannini, Claudio, Tommaso Massai, Antonino Maria Marra, and Gianni Bartoli. "Interference of vortex-induced vibration and galloping: Experiments and mathematical modelling." *Procedia engineering* 199 (2017): 3133-3138.
- [13] Young, Terry, Mari Palta, Jerome Dempsey, James Skatrud, Steven Weber, and Safwan Badr. "The occurrence of sleep-disordered breathing among middle-aged adults." *New England Journal of Medicine* 328, no. 17 (1993): 1230-1235.
- [14] Huang, L. "Flutter of cantilevered plates in axial flow." *Journal of Fluids and Structures* 9 (1995): 127-147.
- [15] Bertram, Christopher D. "Flow-induced oscillation of collapsed tubes and airway structures." *Respiratory Physiology and Neurobiology* 163, no. 1-3 (2008): 256-265.
- [16] Cook, Robert D. "Beam cantilevered from elastic support: Finite-element modelling." *Communications in Applied Numerical Methods* 7, no. 8 (1991): 621-623.
- [17] Rodenstein, Daniel O., Georges Dooms, Yves Thomas, Giuseppe Liistro, Dan C. Stanescu, C. Culee, and Genevieve Aubert-Tulkens. "Pharyngeal shape and dimensions in healthy subjects, snorers, and patients with obstructive sleep apnoea." *Thorax* 45, no. 10 (1990): 722-727.
- [18] Yucel, Aylin, Mehmet Unlu, Alpay Haktanir, Murat Acar, and Fatma Fidan. "Evaluation of the upper airway cross-sectional area changes in different degrees of severity of obstructive sleep apnea syndrome: cephalometric and dynamic CT study." *American journal of neuroradiology* 26, no. 10 (2005): 2624-2629.
- [19] Pelteret, J. P.V., and B. D. Reddy. "Computational model of soft tissues in the human upper airway." *International Journal for Numerical Methods in Biomedical Engineering* 28, no. 1 (2012): 111-132.
- [20] Brown, I. G., T. D. Bradley, E. A. Phillipson, N. Zamel, and V. Hoffstein. "Pharyngeal compliance in snoring subjects with and without obstructive sleep apnea." *Am Rev Respir Dis* 132, no. 2 (1985): 211-215.
- [21] Aurégan, Y. and C. Depollier. "Snoring: Linear stability analysis and in-vitro experiments." *Journal of Sound and Vibration* 188, no. 1 (1995): 39-53.
- [22] Huang, Lixi, and Chao Zhang. "Modal analysis of cantilever plate flutter." *Journal of Fluids and Structures* 38 (2013): 273 - 289.
- [23] Guo, C. Q., and M. P. Paidoussis. "Stability of rectangular plates with free side-edges in two-dimensional inviscid channel flow." *Journal of Applied Mechanics* 67, no. 1 (2000): 171-176.
- [24] Tang, Liaosha, and Michael P. Paidoussis. "On the instability and the post-critical behaviour of two-dimensional cantilevered flexible plates in axial flow." *Journal of Sound and Vibration* 305, no. 1-2 (2007): 97-115.
- [25] Tang, Liaosha, and Michael P. Paidoussis. "The influence of the wake on the stability of cantilevered flexible plates in axial flow." *Journal of Sound and Vibration* 310, no. 3 (2008): 512-526.
- [26] Shoele, Kourosh, and Rajat Mittal. "Flutter instability of a thin flexible plate in a channel." *Journal of Fluid Mechanics* 786 (2016): 29-46.
- [27] Balint, T. S., and A. D. Lucey. "Instability of a cantilevered flexible plate in viscous channel flow." *Journal of Fluids and Structures* 20, no. 7 (2005): 893-912.
- [28] Tetlow, G. A., and A. D. Lucey. "Motions of an offset plate in Viscous channel flow: A model for flutter of the soft palate." In *World Congress on Medical Physics and Biomedical Engineering 2006*, pp. 3457-3460. Springer, Berlin, Heidelberg, 2007.
- [29] Tetlow, G. A., and Anthony D. Lucey. "Motions of a cantilevered flexible plate in viscous channel flow driven by a constant pressure drop." *Communications in numerical methods in engineering* 25, no. 5 (2009): 463-482.
- [30] Howell, R. M., A. D. Lucey, P. W. Carpenter, and M. W. Pitman. "Interaction between a cantilevered-free flexible plate and ideal flow." *Journal of Fluids and Structures* 25, no. 3 (2009): 544-566.
- [31] Burke, Meagan A., Anthony D. Lucey, Richard M. Howell, and Novak SJ Elliott. "Stability of a flexible insert in one wall of an inviscid channel flow." *Journal of Fluids and Structures* 48 (2014): 435-450.
- [32] Khalili, Mohammadtaghi, Martin Larsson, and Bernhard Müller. "Interaction between a simplified soft palate and compressible viscous flow." *Journal of Fluids and Structures* 67 (2016): 85-105.
- [33] Mesquita, J., J. Fiz, J. Solá-Soler, J. Morera, and R. Jan. "Regular and non regular snore features as markers of SAHS." In *32nd Annual International Conference of the IEEE EMBS*, Buenos Aires, Argentina, (2010): 6138-6141.
- [34] Cavusoglu, M., T. Ciloglu, Y. Serinagaoglu, M. Kamasak, O. Eroglu, and T. Akcam. "Investigation of sequential properties of snoring episodes for obstructive sleep apnoea identification." *Physiological Measurement* 29, no. 8 (2008): 879-898.
- [35] Abeyratne, Udantha R., Ajith S. Wakwella, and Craig Hukins. "Pitch jump probability measures for the analysis of snoring sounds in apnea." *Physiological measurement* 26, no. 5 (2005): 779.

- [36] Solá-Soler, J., R. Jan, J. Fiz, and J. Morera. "Automatic classification of subjects with and without sleep apnea through snoring analysis." In *Proceedings of the 29th Annual International Conference of the IEEE EMBS*, Cit Internationale, Lyon, France, (2007): 6093–6096.
- [37] Lee, T. H., Udantha Ranjith Abeyratne, Kathiravelu Puvanendran, and K. L. Goh. "Formant-structure and phase-coupling analysis of human snoring sounds for the detection of obstructive sleep apnea." *Computer Methods in Biomechanics and Biomedical Engineering-3* (2001): 243-248.
- [38] Dalmaso, F., and R. Prota. "Snoring: analysis, measurement, clinical implications and applications." *European Respiratory Journal* 9, no. 1 (1996): 146-159.
- [39] Moretti, Peter M. "Tension in fluttering flags." *International Journal of Acoustics and Vibration* 8, no. 4 (2003): 227–230.
- [40] Gerstenberger, Axel, and Wolfgang A. Wall. "Enhancement of fixed-grid methods towards complex fluid–structure interaction applications." *International Journal for Numerical Methods in Fluids* 57, no. 9 (2008): 1227-1248.
- [41] Degroote, Joris, Abigail Swillens, Peter Bruggeman, Robby Haelterman, Patrick Segers, and Jan Vierendeels. "Simulation of fluid–structure interaction with the interface artificial compressibility method." *International Journal for Numerical Methods in Biomedical Engineering* 26, no. 3-4 (2010): 276-289.
- [42] Oñate, E., M. Cervera, and O. Zienkiewicz. "A finite volume format for structural mechanics." *International Journal for Numerical Methods in Engineering* 37, no. 2 (1994): 181–201.
- [43] Zienkiewicz, O. and R. Taylor. *The Finite Element Method Vol 1: The Basis*. Oxford: Butterworth-Heinemann, 2001.
- [44] Berrabah, H. M., N. Z. Sekrane and B. E. Adda. "Determination of Vibration Characteristics of Carbon Nanobeams." *Journal of Advanced Research Design* 16, no. 1 (2016): 1-14.
- [45] Luo, X. Y., and T. J. Pedley "The effects of wall inertia on flow in a two-dimensional collapsible channel." *Journal of Fluid Mechanics* 363 (1998): 253–280.
- [46] Clark, Susanne A., Christine R. Wilson, Makoto Satoh, David Pegelow, and Jerome A. Dempsey. "Assessment of inspiratory flow limitation invasively and noninvasively during sleep." *American Journal of Respiratory and Critical Care Medicine* 158, no. 3 (1998): 713–722.
- [47] Barrera, Jose E., Candace Y. Pau, Veronique-Isabelle Forest, Andrew B. Holbrook, and Gerald R. Popelka. "Anatomic measures of upper airway structures in obstructive sleep apnea." *World Journal of Otorhinolaryngology - Head and Neck Surgery* 3, no. 2 (2017): 85–91.
- [48] Fenn, W. and H. Rahn. *Handbook of Physiology: Respiration*. Washington: American Physiological Society, 1964.